

## Cell-Associated Glucans of *Burkholderia solanacearum* and *Xanthomonas campestris* pv. *citri*: a New Family of Periplasmic Glucans

PHILIPPE TALAGA,<sup>1</sup> BERND STAHL,<sup>2†</sup> JEAN-MICHEL WIERUSZESKI,<sup>3</sup> FRANZ HILLENKAMP,<sup>2</sup>  
SHINJI TSUYUMU,<sup>4</sup> GUY LIPPENS,<sup>3</sup> AND JEAN-PIERRE BOHIN<sup>1\*</sup>

*Laboratoire de Chimie Biologique, Centre National de la Recherche Scientifique UMR 111, Université des Sciences et Technologies de Lille, 59655 Villeneuve d'Ascq Cedex,<sup>1</sup> and Centre National de la Recherche Scientifique URA 1309, Institut Pasteur de Lille, 59019 Lille Cedex,<sup>3</sup> France; Institut für Medizinische Physik und Biophysik, Universität Münster, D-48149 Münster, Germany<sup>2</sup>; and Faculty of Agriculture, Shizuoka University, 836 Ohya, Shizuoka 422, Japan<sup>4</sup>*

Received 17 November 1995/Accepted 29 January 1996

The cell-associated glucans produced by *Burkholderia solanacearum* and *Xanthomonas campestris* pv. *citri* were isolated by trichloroacetic acid treatment and gel permeation chromatography. The compounds obtained were characterized by compositional analysis, matrix-assisted laser desorption ionization mass spectrometry, and high-performance anion-exchange chromatography. *B. solanacearum* synthesizes only a neutral cyclic glucan containing 13 glucose residues, and *X. campestris* pv. *citri* synthesizes a neutral cyclic glucan containing 16 glucose residues. The two glucans were further purified by high-performance anion-exchange chromatography. Methylation analysis revealed that these glucans are linked by 1,2-glycosidic bonds and one 1,6-glycosidic bond. Our 600-MHz homonuclear and <sup>1</sup>H-<sup>13</sup>C heteronuclear nuclear magnetic resonance experiments revealed the presence of a single  $\alpha$ -1,6-glycosidic linkage, whereas all other glucose residues are  $\beta$ -1,2 linked. The presence of this single  $\alpha$ -1,6 linkage, however, induces such structural constraints in these cyclic glucans that all individual glucose residues could be distinguished. The different anomeric proton signals allowed complete sequence-specific assignment of both glucans. The structural characteristics of these glucans contrast with those of the previously described osmoregulated periplasmic glucans.

Cell surface carbohydrates are involved in bacterium-plant interactions in both pathogenesis and symbiosis (6, 7, 15, 16). Three fundamentally distinct categories of carbohydrate structures can be observed in gram-negative bacteria: exopolysaccharides can form a cell-associated capsule or a fluidal slime, lipopolysaccharides are an intrinsic part of the outer membrane, and osmoregulated periplasmic glucans (OPG) were only recently recognized as general constituents of the gram-negative envelopes and are particularly abundant when the medium osmolarity is low. The latter compounds were essentially studied in members of the family *Rhizobiaceae*, where they are known as cyclic  $\beta$ -glucans (6).

A number of studies have demonstrated that *Agrobacterium* and *Rhizobium* species synthesize OPG with similar structures (for reviews, see references 6 and 12). In both genera, OPG are composed of a cyclic  $\beta$ -1,2-linked backbone containing 17 to 40 glucose residues which can be substituted by *sn*-1-phosphoglycerol (20), as well as by methylmalonic acid or succinic acid (13). OPG-defective mutants of *Rhizobium meliloti* form ineffective white pseudonodules on alfalfa (11), and OPG-defective mutants of *Agrobacterium tumefaciens* are avirulent (28). Extracts of *Bradyrhizobium* spp. revealed the presence of cyclic OPG linked by both  $\beta$ -1,3- and  $\beta$ -1,6-glycosidic bonds, containing 10 to 13 glucose residues (21), which can be substituted by phosphocholine (29). OPG-defective mutants of *Bradyrhizobium japonicum* formed ineffective nodules on soybean plants (5). Several researchers have emphasized the cyclic character of these OPG, which was supposed to permit inclusion complexes

with hydrophobic guest molecules (6). This property could be essential for efficient interaction with the host plant.

In a recent study, we have shown that OPG of an unrelated phytopathogenic bacterium, *Pseudomonas syringae* pv. *syringae*, are essentially different from OPG of members of the family *Rhizobiaceae* (32). *P. syringae* synthesizes acyclic, unsubstituted OPG which range from 6 to 13 glucose residues, with the principal species containing 9 glucose residues. The structure is highly branched, and the backbone consists of  $\beta$ -1,2-linked glucose units to which the branches are attached by  $\beta$ -1,6 linkages (32). These OPG play a role in the plant infection process of this bacterium, as genes at the *hrpM* locus, governing OPG biosynthesis, are required for both the expression of disease symptoms on *Phaseolus vulgaris*, the common bean, and development of the hypersensitive reaction on non-host plants (18, 23). These OPG are very similar to those previously described as membrane-derived oligosaccharides in *Escherichia coli* by Kennedy and coworkers (14), and OPG-biosynthetic gene sequences are highly conserved between *E. coli* and *P. syringae* (17).

This observation opened the question of the degree of diversity of OPG structures among bacteria. Many phytopathogenic bacteria are pseudomonads, a group of bacteria of which the representative genus, *Pseudomonas*, is itself very heterogeneous (24). Structural characterization of the OPG synthesized by these bacteria is an essential prerequisite in the establishment of their potential roles in the development of the pathogenesis pathway. In a first attempt, two species were chosen because of similarities in their virulence characteristics despite their different taxonomic positions: in *P.* (now *Burkholderia*) *solanacearum* and *Xanthomonas campestris* pv. *citri*. Amemura and Cabrera-Crespo (1), researchers, had previously reported the presence in the low- $M_r$  neutral polysaccharides of several strains of *X. oryzae*, *X. phaseoli*, and *X. campestris* of cyclic  $\beta$ -1,2

\* Corresponding author. Phone: 20 43 65 92. Fax: 20 43 65 55. Electronic mail address: BOHIN@CITI2.FR.

† Present address: Milupa GmbH & Co. KG, Research International, D-61381 Friedrichsdorf, Germany.

glucans with a 1,6 linkage. Moreover, those researchers had described a glucan with a degree of polymerization of 16 and one  $\alpha$  linkage in *X. oryzae*. We confirmed these observations in a different strain of *X. campestris* and established through high-resolution nuclear magnetic resonance (NMR) analysis the complete sequence of the glucose residues. We report here the cell-associated character of this glucan and that *B. solanacearum* synthesizes a similar but distinct glucan structure containing only 13 units.

(A preliminary report of this work has appeared previously [15a].)

## MATERIALS AND METHODS

**Bacterial strains and growth.** *B. solanacearum* T11 (4) and *X. campestris* pv. citri N1 were from the culture collection of the Laboratory of Plant Pathology, Faculty of Agriculture, Shizuoka University, Shizuoka, Japan. They were grown in LOS (low-osmolarity) medium (32) at 24°C with agitation.

**Isolation and purification of cell-associated oligosaccharides.** Bacteria were collected during the early exponential phase of growth by centrifugation at 4°C for 15 min at  $8,000 \times g$ . Cell pellets were extracted with 5% trichloroacetic acid, and the trichloroacetic acid extracts were neutralized with ammonium hydroxide and desalted on a Sephadex G-15 column. The desalted material was then fractionated by gel filtration on a Bio-Gel P-6 column (Bio-Rad). The column (60 by 1.6 cm) was eluted at room temperature with 0.5% acetic acid at a flow rate of 15 ml/h, and 2.5-ml fractions were collected. The oligosaccharides emerged in a peak with an intermediate weight detected by the phenol-sulfuric acid procedure (8). Fractions containing oligosaccharides were pooled and lyophilized.

**Matrix-assisted laser desorption-ionization (MALDI)-mass spectrometry (MS).** MALDI-MS experiments were carried out on a VISION 2000 (Finnigan MAT, Bremen, Germany) time-of-flight mass spectrometer equipped with a nitrogen laser (337-nm wavelength, 3-ns pulse width). After selection of the appropriate site on the target by microscope, the laser light was focused onto the sample-matrix mixture at an angle of 15° and a power level of  $10^6$  to  $10^7$  W/cm<sup>2</sup>. Positive ions were extracted by a 5- to 10-keV acceleration potential, focused by a lens, and mass separated in a Reflectron time-of-flight instrument. At the detector, ions were postaccelerated to 20 keV for maximum detection efficiency. The resulting signals were recorded with a fast transient digitizer with a maximum channel resolution of 2.5 ns and transferred to a personal computer for accumulation, calibration, and storage. All MALDI mass spectra are the result of 20-single-shot accumulations.

2,5-Dihydroxybenzoic acid (31), the most effective matrix for this compound class, was used in all cases (10 g/liter in water). Lyophilized oligosaccharide samples were redissolved in doubly distilled water and then diluted with an appropriate volume of the matrix solution (1:5, vol/vol). One microliter of the resulting solution was deposited onto a stainless steel target, and the solvent was evaporated under a gentle stream of warm air.

**High-performance anion-exchange chromatography with pulsed amperometric detection.** Analysis of oligosaccharides was performed on a CarboPac PA-100 anion-exchange column (4 by 250 mm; Dionex, Sunnyvale, Calif.) equipped with a CarboPac PA guard column (3 by 25 mm; Dionex). Oligosaccharides were detected with a PAD II pulsed amperometric detector with a gold electrode (Dionex). The following pulse potentials and durations were used for detection:  $E_1$ , 0.05 V ( $t_1$ , 300 ms);  $E_2$ , 0.60 V ( $t_2$ , 120 ms);  $E_3$ , -0.60 V ( $t_3$ , 300 ms). The chromatographic data were integrated and plotted with an SP 4270 integrator (Spectra-Physic, San Jose, Calif.). Oligosaccharides were eluted at a flow rate of 1 ml/min by a two-step procedure consisting of (i) 0.05 M sodium acetate in 0.15 M NaOH for 5 min and (ii) a linear gradient of 0.05 to 0.2 M sodium acetate in 0.15 M NaOH for 35 min. After every run, the column was re-equilibrated in 0.05 M NaOH in 0.15 M NaOH for 15 min.

Preparation of the oligosaccharides was done in a similar way on a CarboPac PA-1 column (10 by 250 mm) at a flow rate of 2 ml/min. Fractions were collected and separated on an AG 50W-X8 column (5 by 1 cm; H<sup>+</sup> form; 100-200 mesh; Bio-Rad) eluted with water. By this procedure, sodium acetate was converted into acetic acid and NaOH was converted into water. The acetic acid produced by this method was neutralized by NH<sub>4</sub>OH. Some Na<sup>+</sup> was left, which was subsequently removed by desalting on a Bio-Gel P-4 column. The concentration of the contaminating oxidized products was low enough that it did not interfere with the analysis.

**Methylation analysis.** The oligosaccharides were methylated as described by Paz-Parente et al. (26). The methyl ethers were obtained after methanolysis (0.5 M methanol-HCl, 24 h, 80°C) and analyzed as partially methylated methyl glycosides by gas-liquid chromatography (GLC)-MS (9). GLC was performed with a Delsi apparatus with a capillary column (25 m by 0.2 mm) coated with DB-1 (0.5- $\mu$ m film thickness) by applying a temperature gradient of 110 to 240°C at 3°C/min and a helium pressure of 40 kPa. The mass spectra were recorded on a Nermag 10-10B mass spectrometer (Rueil-Malmaison) by using an electron energy of 70 eV and an ionizing current of 0.2 mA.

**NMR spectroscopy.** Prior to NMR spectroscopy analysis, the oligosaccharides

were treated twice with <sup>2</sup>H<sub>2</sub>O at room temperature. After each exchange treatment, the materials were lyophilized. Finally, each sample was redissolved in 0.5 ml of <sup>2</sup>H<sub>2</sub>O (99.96 atom% <sup>2</sup>H; Aldrich) giving 22 and 7 mM solutions for the cell-associated glucans of *B. solanacearum* and *X. campestris* pv. citri, respectively. The NMR experiments were performed on a Bruker DMX-600 Spectrometer controlled with a Silicon Graphics INDY computer and equipped with a triple-resonance <sup>1</sup>H-<sup>13</sup>C-<sup>15</sup>N self-shielded z gradient probe head at a temperature of 28°C. All spectra were recorded without sample spinning. Chemical shifts ( $\delta$ ) were referenced to acetone, the internal standard. Two-dimensional homonuclear COSY (correlation spectroscopy) 90, relayed and double-relayed COSY, TOCSY (total correlated spectroscopy), and NOESY (nuclear Overhauser enhancement spectroscopy) experiments and two-dimensional HSQC (heteronuclear single quantum coherence), HSQC-NOESY, and HSQC-TOCSY experiments were performed by using standard Bruker pulse programs. Spectra were acquired with 1,024 by 256 complex points and transformed after zero filling to 2,048 by 1,024 complex points and multiplication with a  $\pi/3$  shifted squared sine in both dimensions.

HSQC-NOESY experiments were obtained with mixing times of 100 to 300 ms, HSQC-TOCSY experiments were performed with 100- to 200-ms mixing times, and HMBC (heteronuclear multiple bond correlation) experiments were realized with a 100-ms delay for evolution of long-range coupling (<sup>3</sup>J <sup>1</sup>H-<sup>13</sup>C) of 5 Hz.

**Other methods.** Protein concentrations were determined by the method of Lowry et al. (19) with bovine serum albumin as the reference protein. Total carbohydrate concentrations were determined by the phenol-sulfuric acid method of Dubois et al. (8) with D-glucose as the standard. Sugar analysis was carried out by gas-liquid chromatography of trimethylsilyl derivatives of methyl glycosides formed by methanolysis in 0.5 M HCl in methanol at 80°C for 24 h (22). Reducing sugars were measured with the same method after reduction of the oligosaccharides with NaBH<sub>4</sub>. Succinate, glycerol, and total phosphorus were measured as previously described (32).

## RESULTS

### Isolation and characterization of cell-associated glucans.

Cell-associated oligosaccharides were extracted from cells of *B. solanacearum* and *X. campestris* pv. citri which were grown in LOS medium by previously described procedures which involved trichloroacetic acid extraction. This extraction procedure was shown to allow the recovery of more than 90% of <sup>14</sup>C-glucose-labeled membrane-derived oligosaccharides in *E. coli* (data not shown). Fractionation on a Bio-Gel P-6 column allowed the separation of two main sugar-containing compounds (Fig. 1A and B). The compounds eluting at the void volume of the column were probably high-molecular-weight lipo- or exopolysaccharides (32). The second peak represents the cell-associated oligosaccharides. Although the levels of the cell-associated oligosaccharides were similar for both bacteria (23 and 17 mg of equivalent glucose per g of cell protein for *B. solanacearum* and *X. campestris* pv. citri, respectively), the elution volumes indicated that the oligosaccharides produced by *B. solanacearum* were smaller than the oligosaccharides produced by *X. campestris* pv. citri. Compositional analysis of the cell-associated oligosaccharides revealed that glucose could account for all of the carbohydrate present, indicating the absence of contaminating lipo- or exopolysaccharide material (data not shown). Further analysis of these samples demonstrated the absence of succinic acid, glycerol, and phosphorus. GLC analysis of the reduced glucans after methanolysis and silylation reactions revealed an absence of detectable reducing glucose within the preparation.

**MALDI-MS.** Quasimolecular ions were obtained by the MALDI-MS method (Fig. 2A and B). Theoretical masses were calculated with unit mass resolution. This analysis for the glucans of *B. solanacearum* gave one quasimolecular ion at  $m/z$  2,129.7 (Fig. 2A), which agrees with the calculated mass for an [M+Na]<sup>+</sup> ion based on an unsubstituted 13-member cyclic glucan. For the glucans of *X. campestris* pv. citri, one quasimolecular ion at  $m/z$  2,616.8 (Fig. 2B) agrees with the calculated mass for an [M+Na]<sup>+</sup> ion based on an unsubstituted 16-member cyclic glucan. No fragment ions were present at the applied laser energy, confirming that MALDI is a very soft desorption-

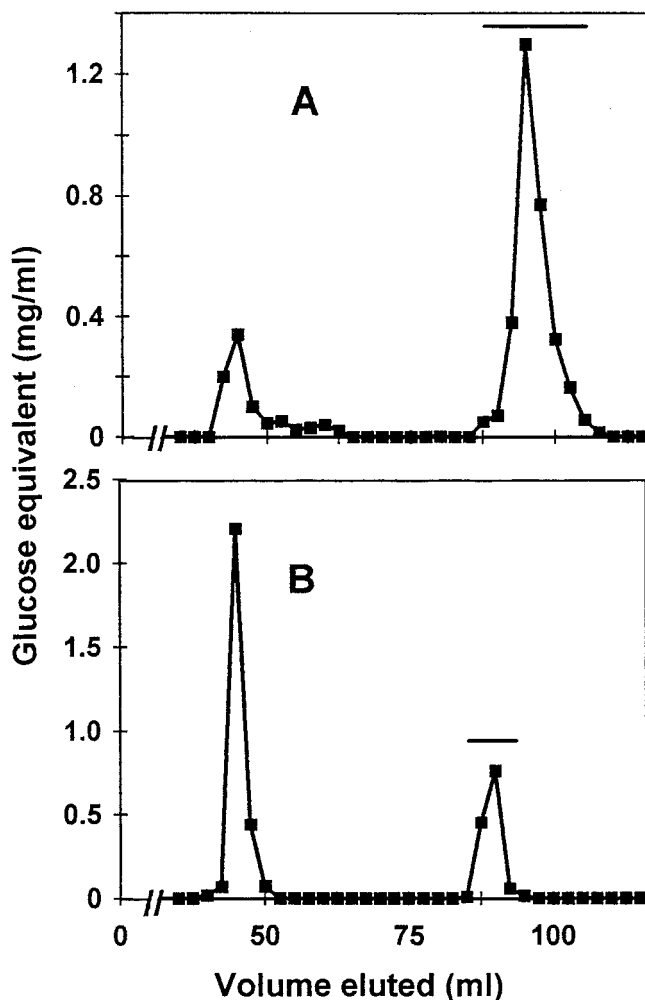


FIG. 1. Bio-Gel P-6 elution profiles of the cell-associated glucans of *B. solanacearum* (A) and *X. campestris* pv. citri (B). The column (1.6 by 60 cm) was eluted with 0.5% acetic acid, and aliquots were analyzed for total carbohydrates (see Materials and Methods). Results are expressed as equivalent glucose milligrams per milliliter of eluant. Fractions indicated by horizontal bars were lyophilized.

ionization technique. Peaks corresponding to the  $[M+K]^+$  ion were also present with  $m/z$  increased by 16 above the masses of the corresponding sodiated ions. This ability to form adduct ions with sodium and potassium has also been observed with the cyclic  $\beta$ -1,2-glucans produced by *R. trifolii* (10). In the *X. campestris* spectrum, cyclic glucans with a higher degree of polymerization (17 to 19 glucose residues per molecule) were detected with extension of the intensity scale by a factor of 20. All of these data indicate that in both cases, the glucan produced is homogeneous in size, in contrast to the previously described osmoregulated periplasmic glucans (6). Preliminary  $^1\text{H}$  NMR analysis confirmed the fact that the glucans produced by *B. solanacearum* and *X. campestris* pv. citri were unsubstituted, but the presence of a low concentration of contaminants forced us to add a second purification step.

**High-performance anion-exchange chromatography-pulsed amperometric detection analysis.** The glucans were analyzed by high-performance anion-exchange chromatography-pulsed amperometric detection on a CarboPac PA-100 column. The chromatograms of the glucans of *B. solanacearum* (Fig. 3A)

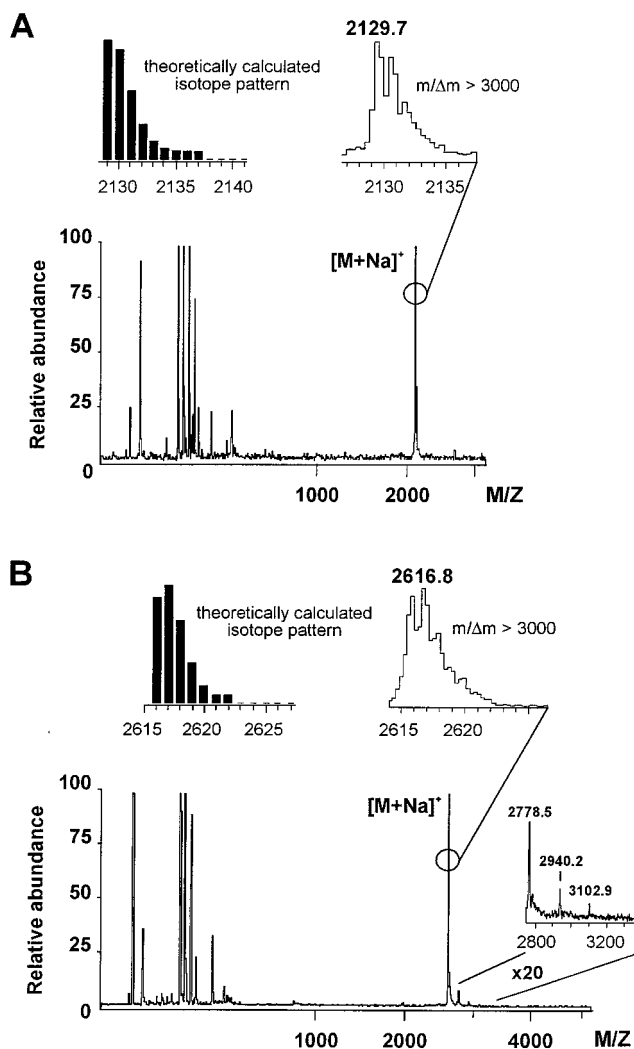


FIG. 2. Positive-ion MALDI mass spectra of the cell-associated glucans of *B. solanacearum* (A) and *X. campestris* pv. citri (B). Mass assignments are based on external calibration. For the most abundant ion, comparison of the theoretically calculated isotope pattern based on an  $[M+Na]^+$  ion with the measured pattern is presented. A scale expanded by a factor of 20 is also shown for the cell-associated glucans of *X. campestris* pv. citri.

and *X. campestris* pv. citri (Fig. 3B) revealed the presence of a major peak in both cases with retention times of 21 and 27 min for the glucans of *B. solanacearum* and *X. campestris* pv. citri, respectively. This analysis confirms the results obtained by MALDI-MS, as in general, the retention time of a homologous series of carbohydrates increases as the degree of polymerization increases. For the glucans of *X. campestris* pv. citri, minor compounds which were eluted later were detected, and they most probably correspond to the higher cyclic glucans observed by MALDI-MS. Further purification of the glucans was performed under the same conditions but with a CarboPac PA-1 preparative column, and the main peak was collected, desalted, lyophilized, and used for structure determination.

**Methylation analysis.** Purified glucans were methylated, methanolized, and, after acetylation, subjected to GLC-MS analysis. Methylation analysis showed the presence of 3,4,6-trimethyl Glc, and 3,4-dimethyl Glc in ratios of 11.8:1 and 15.2:1 for the glucans of *B. solanacearum* and *X. campestris* pv. citri, respectively. These results indicated that the cyclic glu-

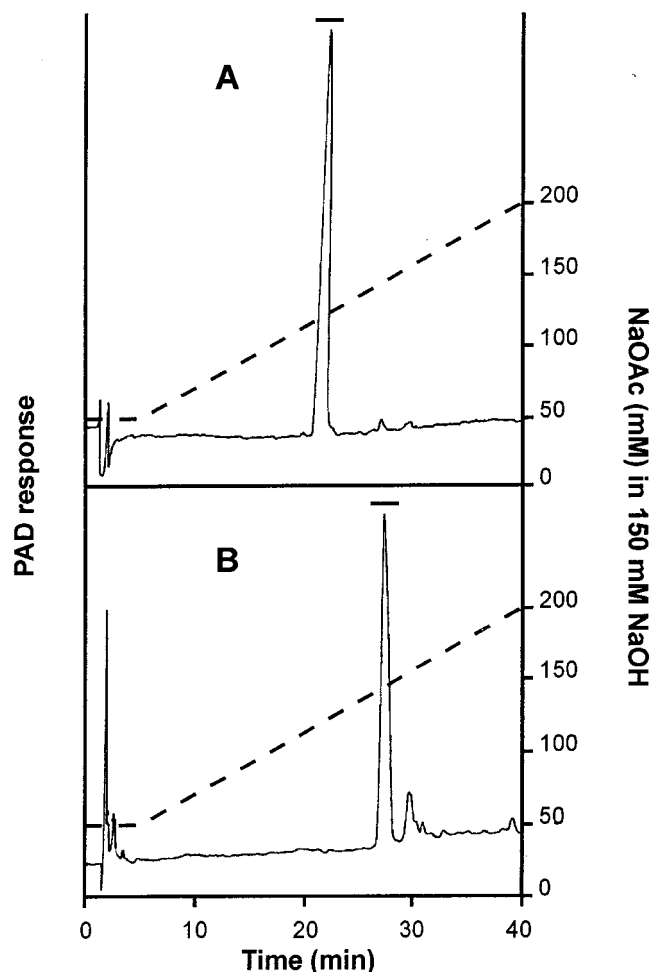


FIG. 3. High-performance anion-exchange chromatography elution profiles of the cell-associated glucans of *B. solanacearum* (A) and *X. campestris* pv. *citri* (B) eluted as described in Materials and Methods. Oligosaccharide peaks were detected by pulsed amperometric detection (PAD). The peaks indicated by horizontal bars were collected, desalted, and lyophilized as described in Materials and Methods. NaOAc, sodium acetate.

cans were composed of one 1,6-linked glucosyl residue with all of the other glucose units joined by 1,2-glycosidic linkages, and the absence of a nonreducing terminal glucose residue suggests that these glucans have no branch point.

**Assignment strategy for NMR analysis.** In the one-dimensional  $^1\text{H}$  NMR spectra, glucose residues were labeled a to m and a to p in decreasing order of the chemical shifts of the H-1 resonances for the cell-associated glucans of *B. solanacearum* and *X. campestris* pv. *citri*, respectively. The  $^1\text{H}$  and  $^{13}\text{C}$  chemical shifts cover relatively small regions of 3.3 to 5.3 ppm for  $^1\text{H}$  and 61 to 105 ppm for  $^{13}\text{C}$ . The assignments of the different protons of every glucose unit were based on COSY 90, relayed COSY, and double-relayed COSY experiments, together with TOCSY experiments. The carbon assignments were based on  $^1\text{H}$ - $^{13}\text{C}$  HSQC and HSQC-TOCSY spectra. The glucose residues were then linked together by a sequential assignment procedure based on the interresidue  $^1\text{H}$ - $^{13}\text{C}$  multiple-bond correlations observed in the HMBC spectra and on the nuclear Overhauser enhancement effects between the H-1 and H-2' protons in HSQC-NOESY experiments.

#### NMR analysis of the cell-associated glucan of *B. solanacearum*.

The  $^1\text{H}$  NMR spectrum (Fig. 4A) shows the presence of a doublet signal at 5.175 ppm with a small coupling constant,  $J_{1,2}$ , of 3.3 Hz that revealed the  $\alpha$ -anomeric configuration of glucose residue a. The other 12 anomeric signals are split by a coupling constant,  $J_{1,2}$ , larger than 7.6 Hz, indicating the  $\beta$ -anomeric configuration of glucose residues b to m. Starting from the anomeric protons, the different homonuclear correlation experiments led to the attribution of all of the proton signals. H-1 and H-2 proton assignments are listed in Table 1. These data were used to extract the carbon frequencies from the HSQC spectrum shown in Fig. 5A. Table 2 contains the C-1 and C-2 values of all of the glucose residues. A small number of resonances attracts special attention. The upfield-shifted cross peaks a3 and a5 (Fig. 5A) confirm the  $\alpha$ -anomeric configuration of residue a. Whereas all C-2 and C-6 resonances fall in the ranges of 80 to 85.2 and 61.5 to 62.5 ppm, respectively, residue f has a C-2 frequency of 74.86 ppm and its H-6 resonances ( $\delta = 3.848$  and 3.901 ppm) correlate with a carbon at 68.95 ppm (cross peaks, f6 and f6'; Fig. 5A). Therefore, residue f has a characteristic upfield-shifted C-2 and a significantly downfield-shifted C-6 ( $\Delta\delta = \sim 7$  ppm). This indicates that this residue has a free OH group at the C-2 position and an OH group at the C-6 position engaged in a glycosidic linkage, in contrast to all of the other glucose residues. Furthermore, the absence of any cross peaks at 92 to 96 ppm in the HSQC spectra, corresponding to C-1 of a reducing glucose residue, confirms the cyclic nature of the glucan.

A sequential assignment procedure was used to link the sugar residues. The observation of a strong cross peak between the anomeric H-1 proton of residue a and the C-6 carbon of residue f (i.e., cross peak aH-1-fC-6) in the HMBC spectrum (Fig. 6A) unambiguously showed that residue a is linked to residue f via an  $\alpha$ -1,6 linkage. Furthermore, the intraresidue contacts H-1-C-3 and H-1-C-5 confirm the  $\alpha$ -anomeric conformation of this residue. For the other glucoses, no such strong intraresidue long-range correlation was observed, confirming the  $\beta$ -anomeric hexapyranoside configuration of these residues. All others HMBC cross peaks linked C-2' to H-1, confirming the  $\beta$ -1,2 linkages. Combining the previously determined H-1 and C-2 attribution with these HMBC cross peaks, a sequential walk through the molecule was established (Fig. 7A).

This primary sequence is in agreement with the nuclear Overhauser enhancement pattern obtained from the HSQC-NOESY experiment (data not shown), in which the cross peaks are no longer based on the long-range coupling constant over the glycosidic linkage but are based on the short H-1-H-2' internuclear distance.

**NMR analysis of the cell-associated glucan of *X. campestris* pv. *citri*.** The  $^1\text{H}$  NMR spectrum of the cell-associated glucan of *X. campestris* pv. *citri* (Fig. 4B) revealed many similarities with the  $^1\text{H}$  NMR spectrum of the cell-associated glucan of *B. solanacearum*. Residue a at 5.172 ppm is in the  $\alpha$ -anomeric configuration ( $J_{1,2} = 3.4$  Hz). The extended spectrum revealed the presence of 15 doublet signals with a coupling constant larger than 7.6 Hz, which indicates the  $\beta$ -anomeric configuration of glucose residues b to p. Attribution of all of the proton signals was done as described above. H-1 and H-2 proton assignments are listed in Table 1. The  $^1\text{H}$ - $^{13}\text{C}$  HSQC spectrum is shown in Fig. 5B. The H-6 and H-6' resonances of residue i were correlated to its C-6 at 68.91 ppm (Fig. 5B), and the C-2 of this residue is characteristically shifted upfield ( $\sim 7$  ppm), indicating that this residue has a free OH group at position C-2. The C-1 and C-2 assignments obtained are listed in Table 2.

The glucose residues were then linked to each other, and the strong cross peak between anomeric H-1 of residue a and C-6 of glucose residue i in the HMBC spectrum (Fig. 6B) reveals

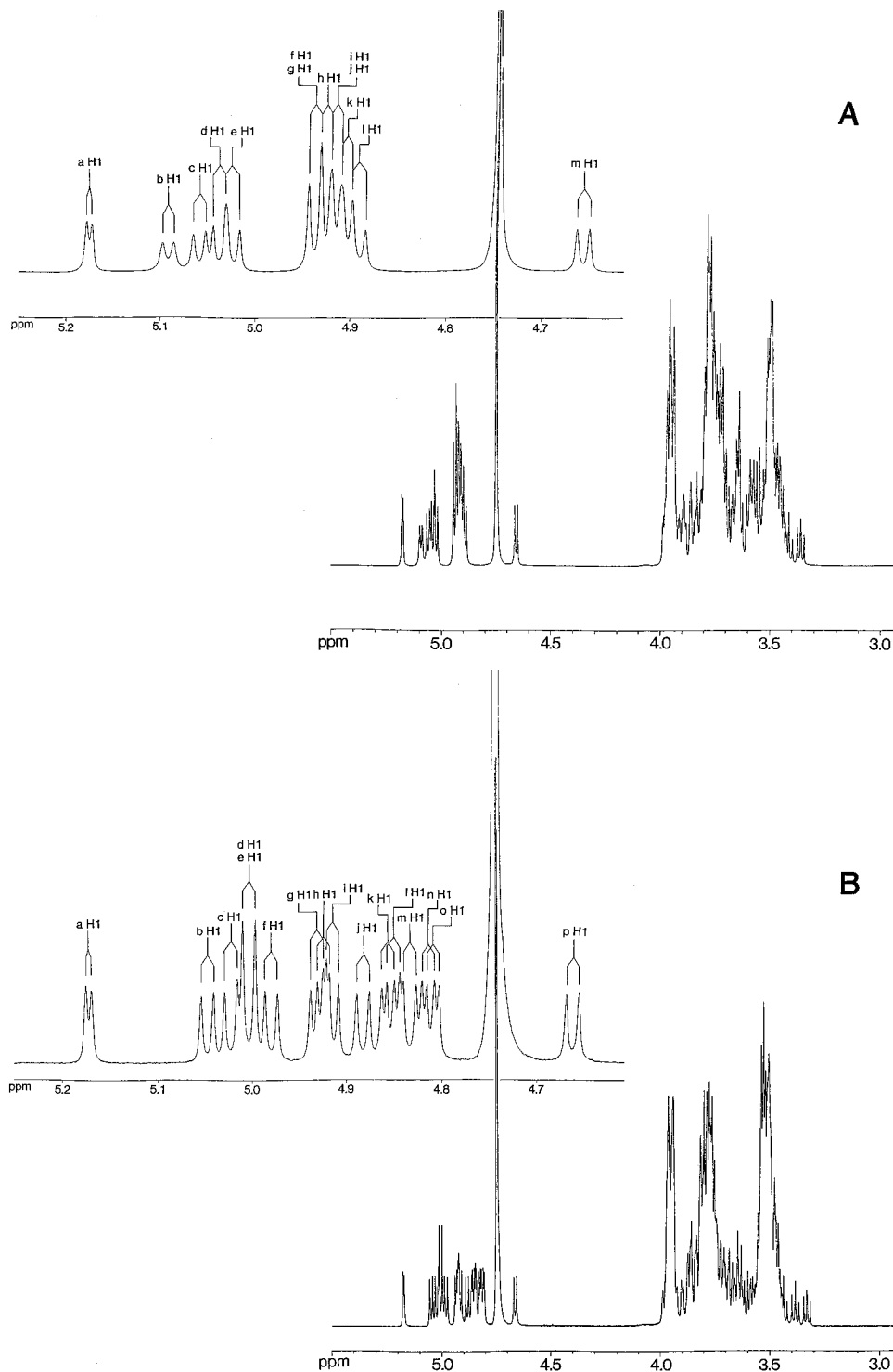


FIG. 4. Six hundred megahertz  $^1\text{H}$  NMR spectra of the cell-associated glucans of *B. solanacearum* (A) and *X. campestris* pv. *citri* (B).

residue a to be linked uniquely to residue i via an  $\alpha$ -1,6 linkage. All of the other glucose residues are linked via  $\beta$ -1,2 glycosidic linkages, as confirmed by the HSQC-NOESY experiment (data not shown).

From analysis of all of the NMR data, the primary structure of the cell-associated glucan of *X. campestris* pv. *citri* was determined as shown in Fig. 7B.

## DISCUSSION

This report describes the structures of glucans extracted from cells of *B. solanacearum* and *X. campestris* pv. *citri* and demonstrates that they are fundamentally different from the major class of previously described OPG of phytopathogenic bacteria. Although they share the cyclic nature with the OPG

TABLE 1. H-1 and H-2 proton chemical shifts of cell-associated glucans<sup>a</sup>

Glucan source	Proton	Chemical shift of each glucose residue (ppm)																
		a	b	c	d	e	f	g	h	i	j	k	l	m	n	o	p	
<i>B. solanacearum</i>	H-1	5.175	5.092	5.059	5.037	5.023	4.935	4.935	4.925	4.915	4.913	4.903	4.891	4.656				
	H-2	3.658	3.716	3.633	3.639	3.712	3.360	3.594	3.699	3.749	3.562	3.694	3.725	3.672				
<i>X. campestris</i> pv. citri	H-1	5.172	5.048	5.022	5.005	5.005	4.981	4.932	4.925	4.915	4.883	4.857	4.851	4.834	4.815	4.810	4.663	
	H-2	3.633	3.577	3.539	3.615	3.541	3.534	3.553	3.586	3.329	3.645	3.704	3.690	3.667	3.682	3.722	3.644	

<sup>a</sup> Chemical shifts relative to acetone (internal reference) are shown.

of members of the family *Rhizobiaceae*, at least three fundamental differences distinguish the two classes of OPG: (i) the molecules described here are restricted to one degree of polymerization (13 for *B. solanacearum* and 16 for *X. campestris* pv. citri), whereas a size distribution appears in the OPG of the *Rhizobiaceae* (ranging from 17 to 25 for *A. tumefaciens*, for example); (ii) they possess a single  $\alpha$ -1,6 linkage, whereas most

previously described OPG are characterized by either a homogeneous  $\beta$ -1,2 linkage pattern or  $\beta$ -1,3 and  $\beta$ -1,6 linkages; and (iii) they exhibit structural rigidity as demonstrated by the distinct chemical shift values of all anomeric protons, whereas NMR studies on the cyclic  $\beta$ -1,2 glucans of *Rhizobium* spp. revealed that all glucopyranosyl residues are magnetically equivalent (2, 27). These differences might all have clear struc-

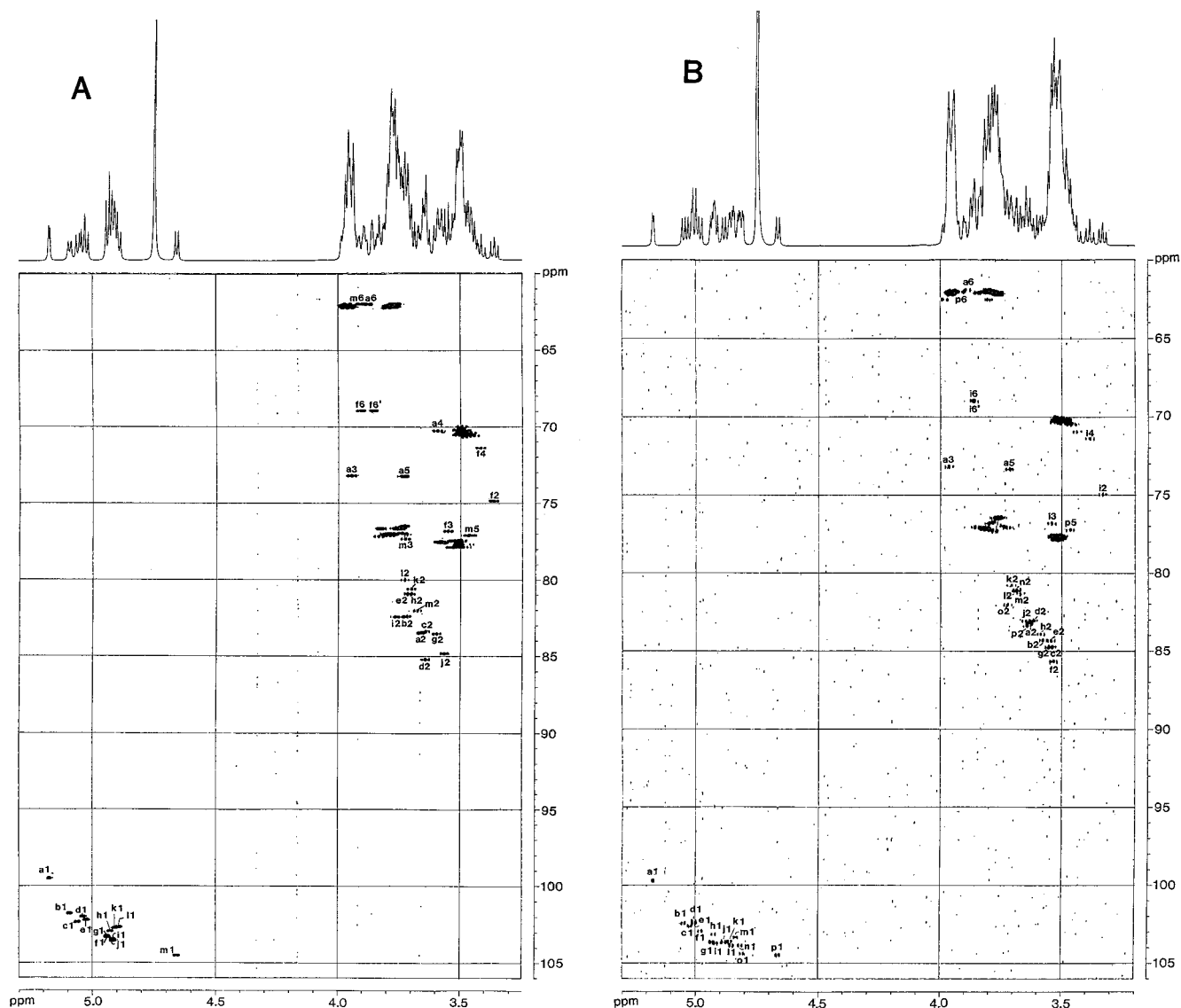


FIG. 5. <sup>13</sup>C-decoupled, <sup>1</sup>H-detected HSQC spectra of the cell-associated glucans of *B. solanacearum* (A) and *X. campestris* pv. citri (B).

TABLE 2. C-1 and C-2 chemical shifts of cell-associated glucans<sup>a</sup>

Glucan source	Carbon	Chemical shift of each glucose residue (ppm)																
		a	b	c	d	e	f	g	h	i	j	k	l	m	n	o	p	
<i>B. solanacearum</i>	C-1	99.48	101.77	102.29	102.00	102.18	103.32	103.30	102.94	103.41	103.54	102.71	102.64	104.52				
	C-2	83.43	82.36	83.36	85.17	80.91	74.86	83.48	81.01	82.42	84.80	80.55	79.96	81.97				
<i>X. campestris</i> pv. citri	C-1	99.69	102.49	102.66	102.37	102.44	102.97	103.66	103.19	103.72	103.64	103.61	103.88	103.34	103.88	104.36	104.70	
	C-2	83.35	84.29	84.77	83.02	84.34	85.62	84.76	83.88	74.93	83.08	80.77	81.16	81.39	81.05	82.02	83.44	

<sup>a</sup> Chemical shifts relative to acetone (internal reference) are shown.

tural and functional implications, which will be discussed below.

The overall ring size distributions of the cyclic  $\beta$ -1,2 glucans were found to be very similar among the different species of the family *Rhizobiaceae* (6). Therefore, it seems unlikely that the cyclic glucan backbones themselves confer specificity during legume nodulation. The unique sizes of the cyclic glucans synthesized by both of the bacteria described in this report might point towards an enhanced specificity in the phytopathogenic character. However, in a previous analysis of glucans containing  $\beta$ -1,2-glycosidic linkages from *X. oryzae* (IFO3312), Amemura and Cabrera-Crespo (1) have shown that the main glucan has a degree of polymerization of 16, is cyclic, and contains one  $\alpha$  linkage and one 1,6-glycosidic linkage. The <sup>1</sup>H and <sup>13</sup>C NMR data revealed strong similarities to those of the cell-associated glucans of *X. campestris* pv. citri described in

this work. Thus, *X. oryzae* synthesizes a cell-associated glucan identical to that of *X. campestris*, and this character appears to be specific for the genus *Xanthomonas* rather than a particular plant-bacterium interaction.

For the cyclic glucans of *A. tumefaciens* with only  $\beta$ -1,2 linkages, the size distribution appears to result from competing elongation and cyclization reactions (33). The unique sizes of the cyclic glucans found in *B. solanacearum* and *X. campestris* pv. citri indicate that there is no such competition but point to a highly specific enzyme responsible for cyclization. Moreover, the active sites of the enzymes involved in the cyclization process are presumably structured such that cyclic glucans of different lengths are accommodated in the two bacteria.

Cyclic  $\beta$ -1,2 glucans with degrees of polymerization below 17 have never been found within rhizobial cultures, perhaps suggesting that such smaller structures are not energetically favor-

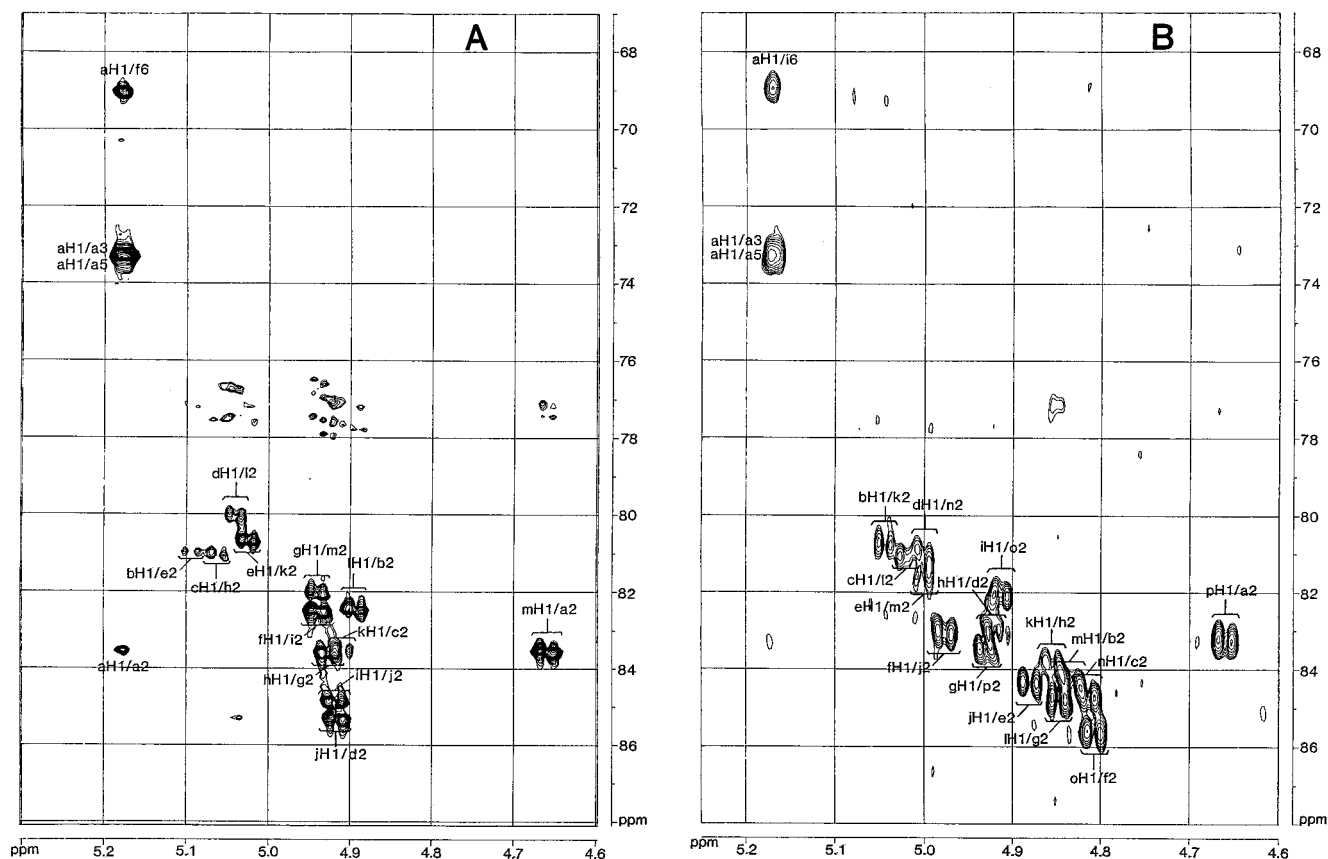


FIG. 6. <sup>1</sup>H-<sup>13</sup>C HMBC spectra of the cell-associated glucans of *B. solanacearum* (A) and *X. campestris* pv. citri (B).

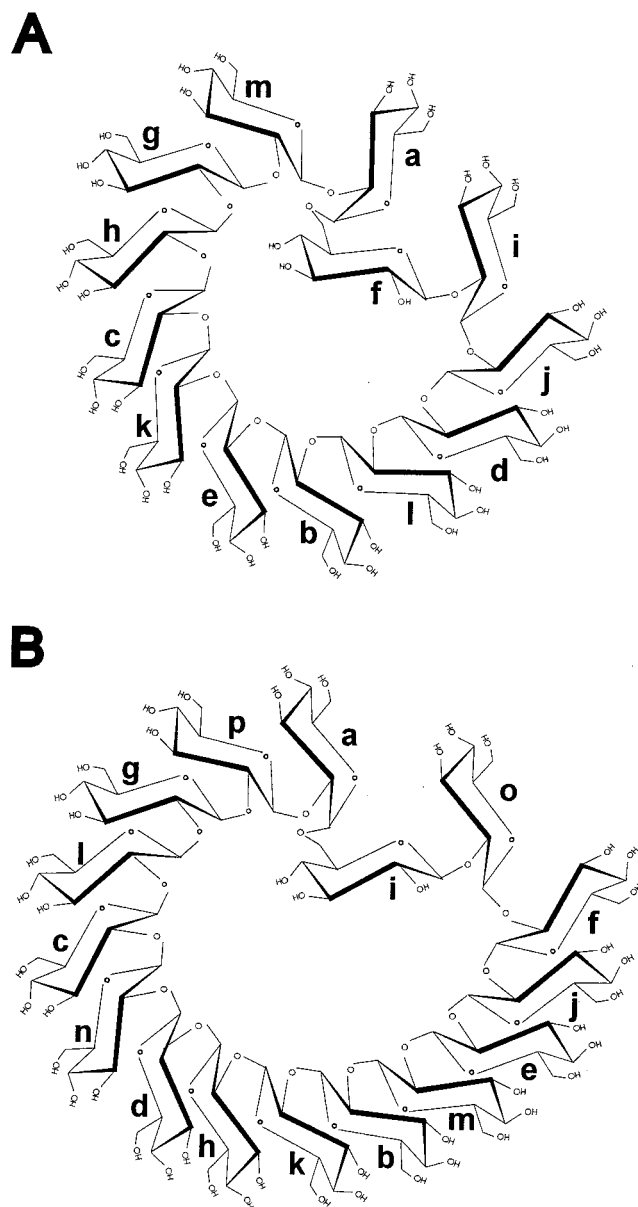


FIG. 7. Primary sequences of the cell-associated glucans of *B. solanacearum* (A) and *X. campestris* pv. *citri* (B). The lowercase letters denote the units in the NMR experiments.

able. This hypothesis was validated by extensive Monte Carlo simulations indicating the unfavorable energetics of such smaller cycles (34). In the molecules described here, the number of units is, in each case, smaller than 17, indicating that the presence of one  $\alpha$ -1,6 linkage relieves, to some extent, the constraint. Even though we do not know whether the  $\alpha$ -1,6 linkage is formed at the initiation, elongation, or cyclization step, the enzymes responsible for the biosynthesis of the cyclic glucans described here have to provide a substantial amount of free energy to obtain a cyclic structure.

Whereas cyclic glucans with only  $\beta$ -1,2 linkages show only six carbon and seven proton resonances, all anomeric proton resonances can be distinguished individually in the two cyclic molecules described in this report. The largest dispersion is found for the H-1 and C-2 resonances, representative of the

successive  $\beta$ -1,2 linkages. André et al. have obtained relaxed conformational maps for  $\beta$ -sophorose by molecular mechanical calculations (3) and considered these zones of low energy as starting models for the conformation of a cyclic  $\beta$ -D-glucan with a degree of polymerization of 17 (2). They arrived at the conclusion of a nonsymmetrical overall shape with a small cavity, in contrast to earlier studies, which proposed a quite regular structure with a large cavity (25, 30). As the chemical shift is a very sensitive probe of the three-dimensional environment of the spin, the different  $\beta$ -1,2 linkages in the OPG of *B. solanacearum* and *X. campestris* pv. *citri* are characterized by different positions in this  $\Phi$ ,  $\Psi$  map without the motional averaging that most probably leads to the unique set of chemical shifts in the  $\beta$ -1,2 glucans. In this respect, it is worth noting that the anomeric protons can be distinguished while no line broadening is observed. This shows that the dynamic averaging in these molecules is limited. A second interesting observation is that the anomeric protons of glucans with degrees of polymerization of 13 and 16 can be divided into different groups:  $\alpha$ -linked residue a; a first group of anomeric protons resonating downfield of 5.0 or 4.95 ppm in the glucan with a degree of polymerization of 13 or 16, respectively; a second group upfield of the same number of parts per million; and the m or p residue that precede the one  $\alpha$ -1,6 linkage in each respective glucan. Further structural studies are required to determine whether the different groups are representative of different low-energy conformations as calculated for  $\beta$ -sophorose and whether the cavity size of these molecules is compatible with a complexing host character.

The present work is the first step toward a precise biochemical definition of the cell-associated glucans of *B. solanacearum* and *X. campestris* pv. *citri*. It demonstrates that future studies on the correlation of cell-associated glucans with virulence will have to take into account the new structural features of these compounds. Additional studies in progress are aimed at further elucidating the cellular location, dependence on medium osmolarity, and detailed molecular modeling of these unusual glucans.

#### ACKNOWLEDGMENTS

We thank Yves Leroy for the GLC-MS analyses and Jianru Stahl-Zeng for recording the MALDI mass spectra of the cell-associated glucan extracted from *B. solanacearum*. We are also grateful to Anne Bohin for excellent technical assistance in the culture of phytopathogenic bacteria.

This work was supported by the Ministère de l'Éducation Nationale and by the CNRS (UMR111 and URA1309). It was performed as a collaborative effort of the Laboratoire Européen Associé "Analyse structure-fonction de biomolécules: approche multidisciplinaire" (CNRS, France-FNRS, Belgium).

#### ADDENDUM IN PROOF

After this article was submitted for publication, an article reporting a structural analysis of the periplasmic glucans produced by *Xanthomonas campestris* was published (W. S. York, Carbohydr. Res. 278:205–225, 1995). This report is in a complete agreement with our conclusions.

#### REFERENCES

- Amemura, A., and J. Cabrera-Crespo. 1986. Extracellular oligosaccharides and low- $M_r$  polysaccharides containing (1,2)- $\beta$ -D-glucosidic linkages from strains of *Xanthomonas*, *Escherichia coli* and *Klebsiella pneumoniae*. J. Gen. Microbiol. 132:2443–2452.
- André, I., K. Mazeau, F. R. Taravel, and I. Tvaroska. 1995. Conformation and dynamics of a cyclic (1,2)- $\beta$ -D-glucan. Int. J. Biol. Macromol. 17:189–198.
- André, I., K. Mazeau, F. R. Taravel, and I. Tvaroska. 1995. NMR and



- molecular modelling of sophorose and sophotriose in solution. *New J. Chem.* **19**:331–339.
4. **Arwiyanto, A., M. Goto, S. Tsuyumu, and Y. Takinawa.** 1994. Biological control of bacterial wilt of tomato by an avirulent strain of *Pseudomonas solanacearum* isolated from *Strelitzia reginae*. *Ann. Phytopathol. Soc. Jpn.* **60**:421–430.
  5. **Bhagwat, A. A., and D. L. Keister.** 1995. Site-directed mutagenesis of the  $\beta$ -(1,3);(1,6)-D-glucan synthesis locus of *Bradyrhizobium japonicum*. *Mol. Plant-Microbe Interact.* **8**:366–370.
  6. **Breedveld, M. W., and K. J. Miller.** 1994. Cyclic  $\beta$ -glucans of the family *Rhizobiaceae*. *Microbiol. Rev.* **58**:145–161.
  7. **Denny, T. P.** 1995. Involvement of bacterial polysaccharides in plant pathogenesis. *Annu. Rev. Phytopathol.* **58**:145–161.
  8. **Dubois, M., K. A. Gilles, J. K. Hamilton, and F. Smith.** 1956. Colorimetric method for determination of sugars and related substances. *Anal. Biochem.* **28**:350–356.
  9. **Fournet, B., G. Strecker, Y. Leroy, and J. Montreuil.** 1981. Gas-liquid chromatography and mass-spectrometry of methylated and acetylated methyl glycosides. Application to the structural analysis of glycoprotein glycans. *Anal. Biochem.* **116**:489–502.
  10. **Garozzo, D., E. Spina, L. Sturiale, G. Montaudo, and R. Rizzo.** 1994. Quantitative determination of  $\beta$ -(1,2) cyclic glucans by matrix-assisted laser desorption mass spectrometry. *Rapid Commun. Mass Spectrom.* **8**:358–360.
  11. **Geremia, R. A., S. Cavaignac, A. Zorreguieta, N. Toro, J. Olivares, and R. A. Ugalde.** 1987. A *Rhizobium meliloti* mutant that forms ineffective pseudo-nodules in alfalfa produces exopolysaccharide but fails to form  $\beta$ -(1 $\rightarrow$ 2) glucan. *J. Bacteriol.* **169**:880–884.
  12. **Hisamatsu, M.** 1992. Cyclic (1,2)- $\beta$ -D-glucan (cyclophorans) produced by *Agrobacterium* and *Rhizobium* species. *Carbohydr. Res.* **231**:137–146.
  13. **Hisamatsu, M., T. Yamada, T. Higashiura, and M. Ikeda.** 1987. The production of acidic, o-acylated cyclophorans [cyclic (1,2)- $\beta$ -D-glucans] by *Agrobacterium* and *Rhizobium* species. *Carbohydr. Res.* **163**:115–122.
  14. **Kennedy, E. P.** 1987. Membrane-derived oligosaccharides, p. 672–679. *In* F. C. Neidhardt, J. L. Ingraham, K. B. Low, B. Magasanik, M. Schaechter, and H. E. Umbarger (ed.), *Escherichia coli* and *Salmonella typhimurium*: cellular and molecular biology. American Society for Microbiology, Washington, D.C.
  15. **Leigh, J. A., and G. C. Walker.** 1994. Exopolysaccharides of *Rhizobium meliloti*: synthesis, regulation and symbiotic function. *Trends Genet.* **10**:63–67.
  - 15a. **Lippens, G., P. Talga, J.-M. Wieruszski, and J.-P. Bohin.** 1995. Structural studies of the osmoregulated periplasmic glucans of *P. solanacearum* and *X. campestris*, p. 423–429. *In* J.-C. Merlin, S. Turrell, and J.-P. Huvenne (ed.), *Spectroscopy of biological molecules*. Kluwer Academic Publishers, Dordrecht, The Netherlands.
  16. **Long, S. R., and B. J. Staskawicz.** 1993. Prokaryotic plant parasites. *Cell* **73**:921–935.
  17. **Loubens, I., L. Debarbieux, A. Bohin, J.-M. Lacroix, and J.-P. Bohin.** 1993. Homology between a genetic locus (*mdoA*) involved in the osmoregulated biosynthesis of periplasmic glucans in *Escherichia coli* and a genetic locus (*hpm*) controlling the pathogenicity of *Pseudomonas syringae*. *Mol. Microbiol.* **10**:329–340.
  18. **Loubens, I., G. Richter, D. Mills, and J.-P. Bohin.** 1994. A pathogenicity gene of *Pseudomonas syringae* pv. *syringae* complements a defect in periplasmic glucan biosynthesis in *Escherichia coli* K12, p. 491–496. *In* M. Lemattre, S. Freigoun, K. Rudolph, and J. G. Swings (ed.), *Plant pathogenic bacteria*. INRA Press, Paris.
  19. **Lowry, O. H., N. J. Rosebrough, A. L. Farr, and R. J. Randall.** 1951. Protein measurement with the Folin phenol reagent. *J. Biol. Chem.* **193**:265–275.
  20. **Miller, K. J., R. S. Gore, and A. J. Benesi.** 1988. Phosphoglycerol substituents present on the cyclic  $\beta$ -1,2-glucans of *Rhizobium meliloti* 1021 are derived from phosphatidylglycerol. *J. Bacteriol.* **170**:4569–4575.
  21. **Miller, K. J., R. S. Gore, R. Johnson, A. J. Benesi, and V. N. Reinhold.** 1990. Cell-associated oligosaccharides of *Bradyrhizobium* spp. *J. Bacteriol.* **172**:136–142.
  22. **Montreuil, J., S. Bouquelet, H. Debray, B. Fournet, G. Spik, and G. Strecker.** 1986. Glycoproteins, p. 143–204. *In* M. F. Chaplin and J. F. Kennedy (ed.), *Carbohydrate analysis: a practical approach*. IRL Press, Inc., Washington, D.C.
  23. **Mukhopadhyay, P., J. Williams, and D. Mills.** 1988. Molecular analysis of a pathogenicity locus in *Pseudomonas syringae* pv. *syringae*. *J. Bacteriol.* **170**:5479–5488.
  24. **Palleroni, N. J.** 1992. Present situation of the taxonomy of aerobic pseudomonads, p. 105–115. *In* E. Galli, S. Silver, and B. Witholt (ed.), *Pseudomonas: molecular biology and biotechnology*. American Society for Microbiology, Washington, D.C.
  25. **Palleschi, A., and V. Crescenzi.** 1985. On a possible conformation of cyclic  $\beta$ (1,2)-D-glucans. *Gazz. Chim. Ital.* **115**:243–245.
  26. **Paz Parente, J., P. Cardon, Y. Leroy, J. Montreuil, B. Fournet, and G. Ricard.** 1985. A convenient method for methylation of glycoproteins glycans in small amounts by using lithium methylsulfinyl carbanion. *Carbohydr. Res.* **141**:41–47.
  27. **Poppe, L., W. S. York, and H. Van Halbeek.** 1993. Measurement of interglycosidic  $^{13}\text{C}$ - $^1\text{H}$  coupling constants in a cyclic  $\beta$ -(1,2)-glucan by  $^{13}\text{C}$ -filtered 2D  $\{^1\text{H}, ^1\text{H}\}$  ROESY. *J. Biomol. NMR* **3**:81–89.
  28. **Puvanesarajah, V., F. M. Schell, G. Stacey, C. J. Douglas, and E. W. Nester.** 1985. Role for 2-linked- $\beta$ -D-glucan in the virulence of *Agrobacterium tumefaciens*. *J. Bacteriol.* **164**:102–106.
  29. **Rolin, D. B., P. E. Pfeffer, S. F. Osman, B. S. Szwegold, F. Kappler, and A. J. Benesi.** 1992. Structural studies of a phosphocholine substituted  $\beta$ -(1,3);(1,6) macrocyclic glucan from *Bradyrhizobium japonicum* USDA 110. *Biochim. Biophys. Acta* **1116**:215–225.
  30. **Serrano, A. M. G., G. Franco-Rodríguez, I. González-Jiménez, P. Tejero-Mateo, J. M. Molina, J. A. Dobado, M. Megias, and M. J. Romero.** 1993. The structure and molecular mechanics calculations of the cyclic (1-2)- $\beta$ -D-glucan secreted by *Rhizobium tropici* CIAT 899. *J. Mol. Struct.* **301**:211–226.
  31. **Stahl, B., M. Steup, M. Karas, and F. Hillenkamp.** 1991. Analysis of neutral oligosaccharides by matrix-assisted laser desorption/ionization mass spectrometry. *Anal. Chem.* **63**:1463–1466.
  32. **Talaga, P., B. Fournet, and J.-P. Bohin.** 1994. Periplasmic glucans of *Pseudomonas syringae* pv. *syringae*. *J. Bacteriol.* **176**:6538–6544.
  33. **Williamson, G., K. Damani, P. Devenney, C. B. Faulds, V. J. Morris, and B. J. H. Stevens.** 1992. Mechanism of action of cyclic  $\beta$ -1,2-glucan synthetase from *Agrobacterium tumefaciens*: competition between cyclization and elongation reactions. *J. Bacteriol.* **174**:7941–7947.
  34. **York, W. S., J. U. Thomsen, and B. Meyer.** 1993. The conformations of cyclic (1-2)- $\beta$ -D-glucans: application of multidimensional clustering analysis to conformational data sets obtained by Metropolis Monte Carlo calculations. *Carbohydr. Res.* **248**:55–80.